Investigative synthesis and optimization of Ca^{2+}/Al^{3+} dual cross-linked alginate hydrogel beads for water vapor adsorption

Tran Thi Khanh Linh[1, 2], Nguyen Thi Huong[1*], Vu Minh Thanh[1]

[1]Institute of Materials, Biology and Environment, Academy of Military Science and Technology, 17 Hoang Sam, Nghia Do, Hanoi, Vietnam;
[2]Vietnam Military Medical Academy, 160 Phung Hung, Ha Dong, Hanoi, Vietnam.
[*]Corresponding author: nguyenhuong0916@gmail.com
Received 2 Feb. 2026; Revised 19 Mar. 2026; Accepted 10 Apr. 2026; Published 25 Apr. 2026.
DOI: https://doi.org/10.54939/1859-1043.j.mst.110.2026.109-116

ABSTRACT

Spherical alginate hydrogel beads simultaneously cross-linked by calcium and aluminium ions were fabricated via extrusion-gelation to investigate their potential for atmospheric water harvesting. Alginate concentration (1–5 wt%) and calcium/aluminium molar ratios (1:1, 1:3, 3:1) were systematically optimized. Scanning electron microscopy demonstrated that 2% alginate with a 1:1 cation ratio yielded the most uniform and porous surface morphology, while elevated aluminium content promoted undesirable surface crystallization. The highest specific surface area was confirmed (15.349 m²/g) for the 1:1 formulation with broad mesopore distribution. Fourier-transform infrared spectroscopy validated calcium-oxygen and aluminium-oxygen cross-links alongside characteristic alginate functional groups, and energy-dispersive X-ray mapping confirmed homogeneous elemental distribution via the egg-box mechanism. Thermogravimetric analysis revealed dehydration at 173.8 °C, alginate pyrolysis total 49.65% mass loss to 700 °C, and approximately 50% thermally stable residue. Water vapor adsorption reached 4.22 g/g at 90% relative humidity and 3.84 g/g at 70%, with over 80% uptake achieved within 15–20 hours. Thermal regeneration retained 92-97% capacity over three cycles, establishing these hydrogels as promising low-cost sorbents for atmospheric water harvesting.

Keywords: Alginate; Multivalent cross-linking; Hydrogel; Water harvesting.

1. INTRODUCTION

Alginate is a natural polysaccharide primarily extracted from brown algae, with a structure consisting of β-D-mannuronic acid (M) and α-L-guluronic acid (G) units arranged in M, G, or MG blocks, conferring its characteristic gel-forming ability upon contact with multivalent ions [1]. Under the influence of multivalent cations such as Ca^{2+} or Al^{3+}, alginate chains undergo ionic cross-linking through a coordination mechanism known as the "egg-box" model, in which the cations serve as bridges between the carboxylate groups ($-COO^-$) of guluronate units on adjacent polymer chains. This cross-linking process leads to the formation of a highly ordered three-dimensional polymer network, thereby yielding hydrogel materials with remarkable mechanical strength and superior water retention capacity [2, 3]. Alginate-based hydrogels are increasingly attracting attention in biomedical, energy, and particularly environmental applications due to their biodegradability, high safety, and tunable properties through the selection of crosslinking agents [4]. In environmental applications, alginate hydrogels demonstrate significant efficacy in water treatment and pollutant adsorption owing to their porous structure, large surface area, and flexible ion-exchange capacity [5, 6]. Research has expanded by developing alginate composites with cellulose, metal oxide particles, polyaniline, or polyacrylamide to enhance structural durability, swelling capacity, and adsorption performance. Meanwhile, alginate hydrogel systems with superior water retention have been noted, expanding their use in agriculture, soil remediation, or natural moisture adsorption systems. The design flexibility and environmental friendliness of alginate provide a critical foundation for the application of hydrogels in atmospheric water harvesting, a promising solution amid escalating water scarcity [7, 8].

The selection and modulation of crosslinking ions play a pivotal role in controlling material properties. Multivalent cations produce marked differences in gel network density, with Al^{3+} ions offering stronger binding and harder gels compared to Ca^{2+} [9, 10]. Simulation and experimental studies have shown that the chemical nature and valence of ions directly influence micro-gel structure, crosslinking degree, and water retention of hydrogels. Furthermore, combining two multivalent cations can yield synergistic effects, forming hybrid networks with higher crosslink density, thereby enhancing water adsorption and stability during reuse [11, 12].

Studies on spherical alginate hydrogels simultaneously crosslinked by the Ca^{2+}-Al^{3+} ion system, particularly for atmospheric water harvesting, remain limited. The optimization of bead synthesis processes, the analysis of the impact of mixed ions on gel structure, the evaluation of water vapor adsorption performance, and the assessment of material reusability over multiple moisture absorption–desorption cycles. Stemming from these observations, this study focuses on synthesizing spherical Alg/$CaCl_2$–$AlCl_3$ hydrogels to (i) characterize material structure, (ii) evaluate water vapor adsorption capacity, and (iii) investigate reusability after multiple cycles. The results are expected to contribute to developing sustainable, low-cost materials for atmospheric water harvesting with high practical potential.

2. EXPERIMENTAL

2.1. Materials

All chemicals used were of analytical grade unless otherwise specified. Sodium Alginate (alginic acid sodium salt from brown algae, Merck) and anhydrous calcium chloride and Aluminium chloride $AlCl_3.6H_2O$ (granular, Merck), which served as the cation (Ca^{2+}, Al^{3+}) source for hydrogel multivalent cross-linking, were used. Deionized (DI) water (TDS < 2) was used as a solvent and for washing. Filter paper (ø 110 mm) was purchased from Whatman Ltd. (UK).

2.2. Experimental methods

The synthesis of multivalent cation-crosslinked alginate material with calcium and aluminium (Alginate/CaAl) was performed similarly to the procedure reported in [13]. Sodium alginate was dissolved in deionized water at concentrations ranging from 1 to 5 wt%, followed by ultrasonication (Sonics & Materials VCX500; 500 W, 20 kHz) for 1 h and continuous stirring at 150 rpm for 24 h to obtain a homogeneous, transparent solution. The alginate solution was then added dropwise into 50 mL of $CaCl_2$/$AlCl_3$ solution at a volume ratio of 1:1 and a flow rate of 3 mL/min, with a total cation concentration of 2 M and investigated Ca^{2+}/Al^{3+} molar ratios of 1:1, 1:3, and 3:1. The resulting material was left undisturbed in the crosslinking solution for 3 h. The hydrogel beads were filtered, washed with distilled water to remove excess surface solution, and vacuum-dried at 40–50 °C for 24 h to yield the final product.

2.3. Characterization of Aglinate/CaAl

The obtained Alginate/CaAl hydrogel particles are spherical in shape, with a diameter of 0.2 ± 0.02 cm, white to pale yellow in color, and their structural characteristics were investigated and evaluated using instrumental analysis methods. Fourier-transform infrared (FT-IR) spectra were recorded using a Bruker EQUINOX 55 spectrometer over the wavenumber range of 400–4000 cm^{-1}. The surface morphology and spatial distribution of silver nanoparticles within the polymer matrix were examined by field-emission scanning electron microscopy (FE-SEM) using a Hitachi S-4800 instrument (Hitachi, Japan). Elemental composition was determined by energy-dispersive X-ray spectroscopy (EDX) integrated with the FE-SEM system, and elemental distribution mapping (EDX mapping) was performed to assess the homogeneity of nanoparticle dispersion across the polymer matrix. Nitrogen adsorption–desorption isotherms were measured at 77 K using a Micromeritics TriStar II 3020 analyzer, and the specific surface area was calculated according to the Brunauer–Emmett–Teller (BET) method.

2.4. Evaluation of the water vapor adsorption capacity of Aglinate/CaAl material

Water vapor adsorption was conducted in a humidity generator at relative humidities (RH) of 70% and 90% for various time intervals within a thermo-hygrostat chamber. After each designated time point, the material mass was measured, and the water vapor adsorption capacity q (g/g) was calculated using the following equation:

$$q = \frac{m_t - m_o}{m_h} \ (g/g)$$

where m_t is the total mass of the material and container after t hours of adsorption (g), m_0 is the total mass of the material and container before adsorption (g), and m_h is the mass of the material (g).

3. RESULTS AND DISCUSSION

3.1. Optimization of hydrogel Aglinate/CaAl synthesis

The effect of alginate (Alg) concentration on the microstructure and morphology (Figure 1), as well as the volume ratio of Ca^{2+}/Al^{3+} ions (Figure 2), was investigated in the hydrogel beads. The effect of alginate (Alg) concentration on the surface morphology of Alg/CaAl hydrogel was investigated at a fixed Ca^{2+}/Al^{3+} solution volume ratio of 1:1. The Alg/CaAl material at 1% Alg concentration exhibited a bumpy surface with initial signs of porosity. Increasing the Alg concentration to 2% and 3% resulted in surfaces that deviated from the flat film observed at 1%, displaying pronounced depressions, pores, and cavities that confirmed enhanced surface porosity [14]. This can be explained by that the metal cations (Ca^{2+}/Al^{3+}) crosslinked with carboxyl groups along the Alg chains, promoting chain expansion and stretching of the Alg film, which increased porosity and disrupted the initial continuous gel film structure [15]. Further elevation of Alg concentration to 4% and 5% led to disrupted morphologies featuring large cavities and deep grooves; at 5% Alg, the surface became nearly flat with multi-directional cracks. These findings demonstrate that a 2% Alg concentration yields a highly porous surface morphology, which is expected to provide a large specific surface area and high adsorption capacity.

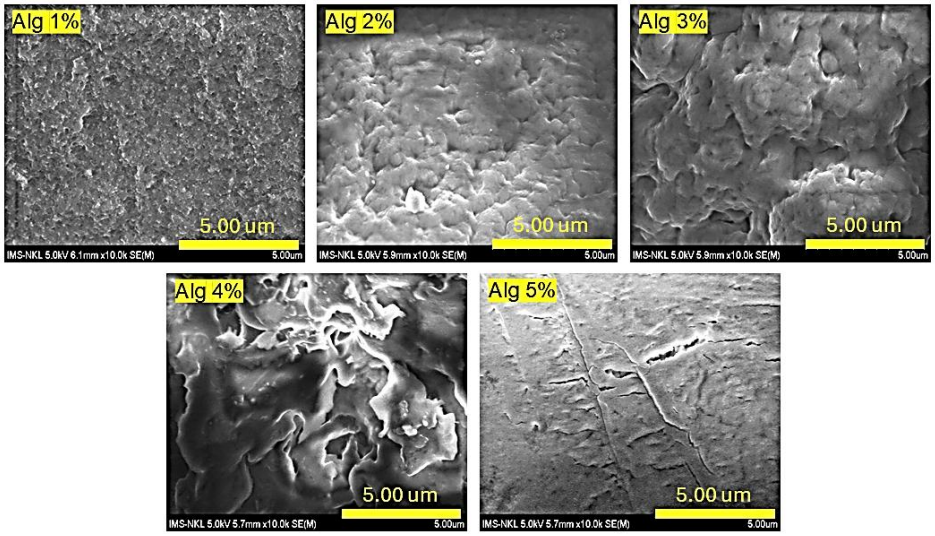

Figure 1. *Morphologies of Alginate/CaAl at different Alginate concentration.*

The influence of cation solution volume ratios (1:1, 1:3, and 3:1) was subsequently examined to identify optimal synthesis conditions, with results presented in Figure 2. Similar to the effects observed with Alg concentration, the three Alg/CaAl samples prepared at different Ca^{2+}/Al^{3+} molar ratios exhibited distinct surface morphologies, particularly in terms of porosity.

The sample with a 1:3 Ca^{2+}/Al^{3+} molar ratio displayed large crystals on a grooved film surface.

In contrast, samples at 1:1 and 3:1 ratios showed no large surface crystals but porous morphologies; however, the 3:1 ratio produced less uniform grooves and pores compared to the 1:1 ratio. These results indicate that varying cation concentrations directly influence surface morphology formation, with high Al^{3+} content promoting crystal development on the Alg film surface [16]. For applications as a water vapor adsorbent for atmospheric water recovery, the 1:1 molar ratio was selected as optimal.

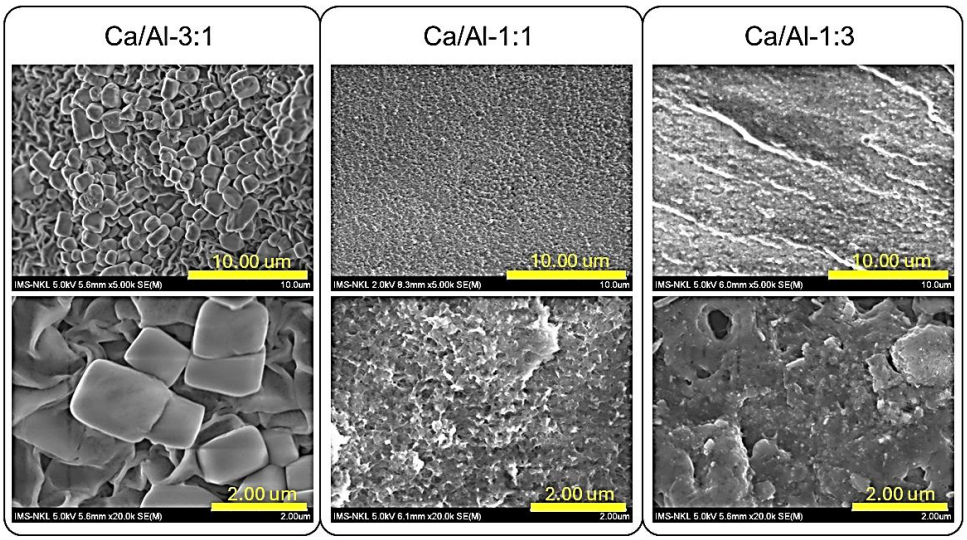

Figure 2. *Morphologies of Alginate/CaAl with a volume ratio of Ca^{2+}/Al^{3+} ions.*

To further elucidate the impact of the cation molar ratios on material porosity, specific surface area was determined via BET analysis, with results shown in Figure 3a. The results of the investigation on the molar ratio of Ca^{2+}/Al^{3+} ions revealed that all three samples exhibited nitrogen adsorption-desorption behavior with noticeable hysteresis loops. However, the shape of the loops and the corresponding relative pressure range (P/P_0) for the adsorption–desorption transitions differed among the samples, representing modified variants of type IV isotherms according to the IUPAC classification. Among them, the Alginate/CaAl sample with a Ca^{2+}/Al^{3+} molar ratio of 1:1 showed a smoother adsorption–desorption curve, and its hysteresis loop extended over a wide relative pressure range ($P/P_0 = 0.1–0.9$), indicating a material with higher porosity and more uniform mesopore size distribution compared to the other two samples [17]. The specific surface areas of the samples with molar ratios of 1:3, 1:1, and 3:1 were 8.849 m^2/g, 15.349 m^2/g, and 4.285 m^2/g, respectively. These results are consistent with the morphological observations of the materials.

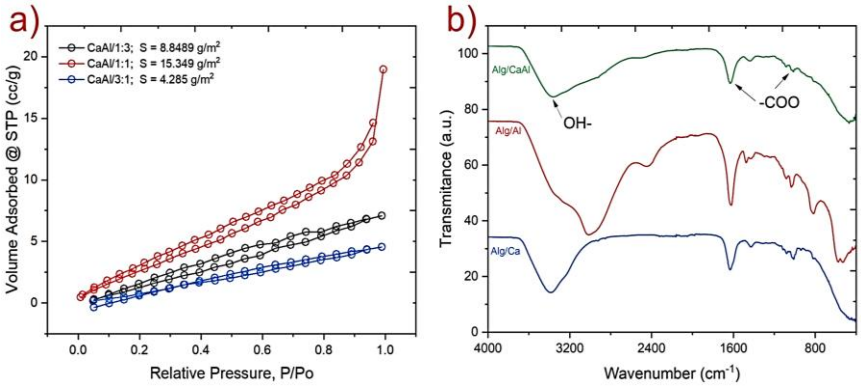

Figure 3. *(a) BET of Alg/CaAl and (b) FTIR spectrum of Alg/Ca, Alg/Ca, and Alg/CaAl composites.*

Structural Characterization of hydrogel Alginate/CaAl:

The FT-IR spectrum of the material (Figure 3b) exhibits characteristic absorption bands. The FT-IR absorbance spectra for Alg-Ca (blue), Alg-Al (red), and Alg-Ca/Al (green) composites display signature bands diagnostic of their chemistry. A wide absorption envelope at 3100-3550 cm^{-1}, peaking ~3320-3360 cm^{-1} across traces (strongest in Alg-Al), arises from O-H stretches of alginate hydroxyls and bound water. Distinct minima near 1595-1620 cm^{-1} reflect overlapping asymmetric COO^- deformation (~1605-1615 cm^{-1}) and H-O-H bending of hydrated layers, underscoring moisture retention linked to $CaCl_2$ hygroscopy, particularly pronounced in Alg-Ca/Al [18]. Additionally, symmetric COO^- modes at ~1410-1420 cm^{-1} and C-O saccharide vibrations ~1030 cm^{-1} persist, while 400-600 cm^{-1} features Ca-O (~590 cm^{-1}, Alg-Ca), Al-O (~460-520 cm^{-1}, Alg-Al), and merged in Alg-Ca/Al verify cation-alginate cross-links [19, 20].

SEM-EDX elemental mapping of 2% Alginate/CaAl (Figure 4a, b). It revealed a uniform distribution of oxygen (O Ka1) and calcium (Ca Ka1), Al (Ka1) across the hydrogel surface, confirming successful formation of calcium alginate networks through ionic crosslinking mechanisms [21]. The sparse distribution of carbon (C Ka1_2) and minimal presence of sodium (Na Ka1_2) and chlorine (Cl Ka1) indicated effective multivalent ion exchange during gelation, where Ca^{2+}/Al^{3+} ions replaced Na^+ ions in the alginate matrix. The corresponding EDX spectrum (demonstrated characteristic peaks for Cl (~2.6 keV) and Ca (~3.7 keV), Al (1,7 KeV), with lower intensity signals for C, O, and Na, consistent with the chemical composition of calcium alginate hydrogels formed via the "egg-box" model crosslinking mechanism [22]. The Ca/Cl and Al/Cl peak intensity ratio and elemental distribution patterns confirmed the structural integrity and homogeneous crosslinking density throughout the alginate/$CaCl_2$ hydrogel matrix, validating successful hydrogel formation through divalent cation coordination with guluronic acid blocks in the alginate backbone [9].

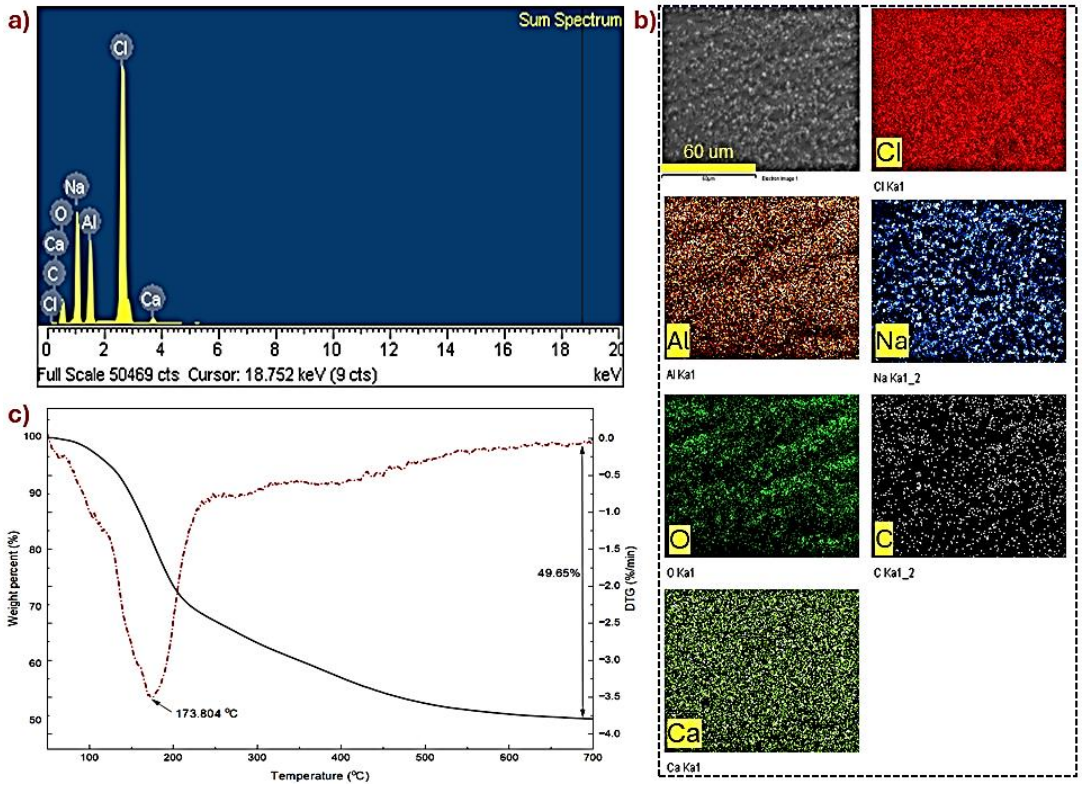

Figure 4. *EDX data (a) and Mapping scan images (b) and DTA-TGA data (c) of Alginate/CaAl.*

TGA profiles (Figure 4c) indicate rapid mass reduction (100 - 250 °C) with a DTG minimum at 173.8 °C, attributable to evaporative loss of free and coordinated water. Subsequent gradual degradation to 700 °C, totaling 49.65% weight loss, corresponds to alginate pyrolysis via glycosidic cleavage and decarboxylation [23]. The substantial residue (~50% at 700 °C) reflects thermal fortification from multivalent ion incorporation, yielding stable metal oxides/char networks [9]. Characteristic DTG peaks validate optimal drying/annealing protocols, preventing premature polymer breakdown during synthesis.

3.2. Water vapor adsorption and regeneration performance

The water vapor adsorption capacity of the Alginate/CaAl material was evaluated under dynamic conditions at two relative humidity (RH) levels: 90% and 70% (Figure 5). The hydrogel's adsorption performance was highly sensitive to relative humidity (RH). Equilibrium uptake reached ~ 4.22 g/g at 90% RH compared to 3.84 g/g at 70% RH. The process exhibited fast initial kinetics, attaining > 80% saturation in 15-20 h and full equilibrium by ~120 h. Reusability tests via thermal regeneration showed modest capacity decline: at 90% RH, from 4.22 g/g (1st cycle) to 4.11 g/g (2nd) and 3.89 g/g (3rd); at 70% RH, from 3.84 g/g (1st cycle) to 3.41 g/g (2nd) and 3.20 g/g (3rd). Equilibrium times remained stable, though reduced capacity likely stems from thermal-induced pore disruption or partial elution of Ca^{2+} cross-links. Replicate experiments showed low variability, with errors of 1.5 - 2.5% in 1st cycle. However, the error increased to 2.0–3.5% in 2nd cycle , suggesting a decline in regeneration efficiency over repeated cycles. Overall, the Alg-Ca/Al composite holds promise for atmospheric water capture owing to its robust humidity-responsive capacity [24].

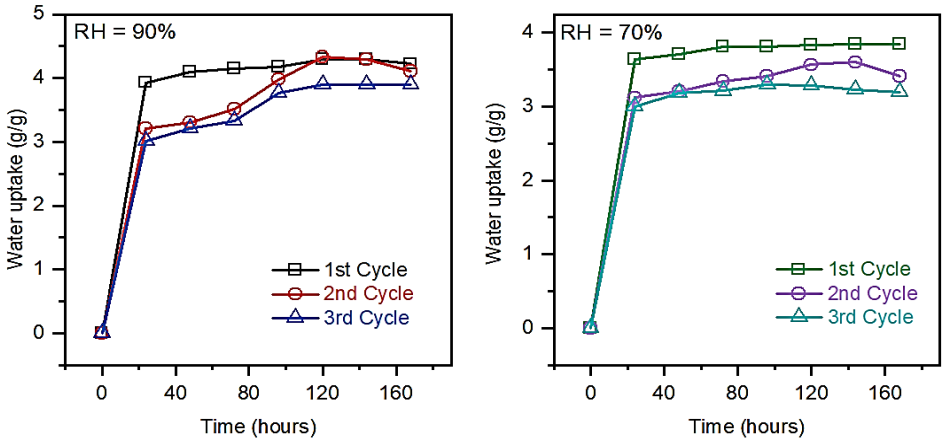

Figure 5. *Water vapor adsorption kinetics of the Alginate/CaAl composite at RH 90% and RH 70%, showing performance during the 1st cycle and after 2 regenerations.*

4. CONCLUSIONS

Dual ionic cross-linking with Ca^{2+}/Al^{3+} proved an effective strategy for engineering porous alginate hydrogels with enhanced hygroscopic performance. The optimal formulation of 2% Alginate/CaAl with a Ca^{2+}:Al^{3+} volume ratio of 1:1 achieved a well-developed porous network while suppressing Al^{3+}-induced crystallization. Multi-technique characterization confirmed cross-link integrity, elemental homogeneity, and thermal stability. Despite modest capacity reduction after regeneration, high reusability and rapid adsorption kinetics support practical deployment in water-scarce environments, providing a rational foundation for biopolymer-based atmospheric water harvesting sorbents. These findings lay a promising foundation for the development of passive, low-cost water harvesting systems deployable in remote, off-grid, or operationally demanding environments, including potential defense and military logistics applications where access to clean water remains a critical challenge.

REFERENCES

[1]. Solberg A., Draget K. I., Schatz C., et al., *"Alginate Blocks and Block Polysaccharides: A Review"*, Macromolecular Symposia, vol. 408, no. 1, (2023).

[2]. Malektaj H., Drozdov A. D., deClaville Christiansen J., *"Mechanical Properties of Alginate Hydrogels Cross-Linked with Multivalent Cations"*, Polymers (Basel), vol. 15, no. 14, (2023).

[3]. Cao L., Lu W., Mata A., et al., *"Egg-box model-based gelation of alginate and pectin: A review"*, Carbohydrate Polymers, vol. 242, (2020).

[4]. Alcalde-Garcia F., Prasher S., Kaliaguine S., et al., *"Desorption Strategies and Reusability of Biopolymeric Adsorbents and Semisynthetic Derivatives in Hydrogel and Hydrogel Composites Used in Adsorption Processes"*, ACS Engineering Au, vol. 3, no. 6, (2023).

[5]. Wang B., Wan Y., Zheng Y., et al., *"Alginate-based composites for environmental applications: A critical review"*, Critical Reviews in Environmental Science and Technology, vol. 49, no. 4, (2018).

[6]. Rana A. K., Gupta V. K., Hart P., et al., *"Cellulose-alginate hydrogels and their nanocomposites for water remediation and biomedical applications"*, Environmental Research, vol. 243, (2024).

[7]. da Costa J. S., de Souza J. F., dos Santos D. R. S., et al., *"Composite aerogels of alginate/poly(acrylamide)/carbon nanotubes with enhanced performance for cationic dyes adsorption"*, Materials Science and Engineering: B, vol. 298, (2023).

[8]. Liang J., Li X., Wu M., et al., *"MXene/polyaniline/sodium alginate composite gel: Adsorption and regeneration studies and application in Cu(II) and Hg(II) removal"*, Separation and Purification Technology, vol. 353, (2025) 128298.

[9]. Brus J., Urbanova M., Czernek J., et al., *"Structure and Dynamics of Alginate Gels Cross-Linked by Polyvalent Ions Probed via Solid State NMR Spectroscopy"*, Biomacromolecules, vol. 18, no. 8, pp. 2478, (2017).

[10]. Ručigaj A., Golobič J., Kopač T., *"The role of multivalent cations in determining the cross-linking affinity of alginate hydrogels: A combined experimental and modeling study"*, Chemical Engineering Journal Advances, vol. 20, (2024).

[11]. Ghanian M. H., Mirzadeh H., Baharvand H., *"In Situ Forming, Cytocompatible, and Self-Recoverable Tough Hydrogels Based on Dual Ionic and Click Cross-Linked Alginate"*, Biomacromolecules, vol. 19, no. 5, pp. 1646, (2018).

[12]. Zhou L., Liu Z., Dai G., et al., *"Experimental research on bimetallic ion crosslinked gel to inhibit the spontaneous combustion of coal"*, Fuel, vol. 357, (2024).

[13]. Nokhodchi A., Tailor A., *"In situ cross-linking of sodium alginate with calcium and aluminum ions to sustain the release of theophylline from polymeric matrices"*, Il Farmaco, vol. 59, no. 12, pp. 999, (2004).

[14]. Fila D., Kołodyńska D., *"Crosslinking agents as precursors for improved selectivity and adsorption performance of alginate hydrogels toward rare earth elements"*, Sustainable Materials and Technologies, vol. 45, (2025).

[15]. Wang Q., Liu S., Wang H., et al., *"In situ pore-forming alginate hydrogel beads loaded with in situ formed nano-silver and their catalytic activity"*, Physical Chemistry Chemical Physics, vol. 18, no. 18, pp. 12610, (2016).

[16]. Hu C., Lu W., Mata A., et al., *"Ions-induced gelation of alginate: Mechanisms and applications"*, International Journal of Biological Macromolecules, vol. 177, (2021).

[17]. Thommes M., Kaneko K., Neimark A. V., et al., *"Physisorption of gases, with special reference to the evaluation of surface area and pore size distribution (IUPAC Technical Report)"*, Pure and Applied Chemistry, vol. 87, no. 9–10, pp. 1051, (2015).

[18]. Larosa C., Salerno M., de Lima J. S., et al., *"Characterisation of bare and tannase-loaded calcium alginate beads by microscopic, thermogravimetric, FTIR and XRD analyses"*, International Journal of Biological Macromolecules, vol. 115, (2018).

[19]. Cho A. R., Chun Y. G., Kim B. K., et al., *"Preparation of alginate–CaCl2 microspheres as resveratrol carriers"*, Journal of Materials Science, vol. 49, no. 13, pp. 4612, (2014).

[20]. Asadi S., Eris S., Azizian S., *"Alginate-Based Hydrogel Beads as a Biocompatible and Efficient Adsorbent for Dye Removal from Aqueous Solutions"*, ACS Omega, vol. 3, no. 11, pp. 15140, (2018).

[21]. Ghaly M., Masry B. A., Abu Elgoud E. M., *"Fabrication of magnesium oxide–calcium alginate hydrogel for scaffolding yttrium and neodymium from aqueous solutions"*, Scientific Reports, vol. 13, no. 1, (2023).

[22]. Kuo C. K., Ma P. X., *"Ionically crosslinked alginate hydrogels as scaffolds for tissue engineering: Part 1. Structure, gelation rate and mechanical properties"*, Biomaterials, vol. 22, no. 6, pp. 511, (2001).
[23]. Wang Z., Liu Y., Li Z., et al., *"Effect of density on the smoldering of calcium alginate fibers"*, RSC Advances, vol. 14, no. 38, pp. 28201, (2024).
[24]. Fu C., Zhan D., Tian G., et al., *"Biomimetic Aerogel Composite for Atmospheric Water Harvesting"*, ACS Applied Materials & Interfaces, vol. 16, no. 27, pp. 35740, (2024).

TÓM TẮT

Nghiên cứu tổng hợp và tối ưu hóa vật liệu hydrogel alginate liên kết chéo Ca^{2+}/Al^{3+} ứng dụng hấp phụ nước từ không khí

Trong nghiên cứu này, các hạt hydrogel alginate hình cầu với liên kết chéo đa hóa trị bởi các cation Ca^{2+} và Al^{3+} được chế tạo bằng phương pháp gel hóa, nhằm đánh giá tiềm năng thu hồi nước trong không khí. Nồng độ alginate (1 - 5% khối lượng) và tỷ lệ mol canxi/nhôm (1:1, 1:3, 3:1) được khảo sát để lựa chọn điều kiện tối ưu cho tổng hợp hydrogel. Kết quả phân tích kính hiển vi điện tử quét cho thấy, mẫu 2% alginate với tỷ lệ cation 1:1 tạo ra hình thái bề mặt đồng đều và xốp nhất, trong khi hàm lượng nhôm cao dẫn đến sự hình thành tinh thể bề mặt không mong muốn. Phổ hồng ngoại biến đổi Fourier cho thấy sự tồn tại của liên kết chéo canxi–oxy và nhôm–oxy cùng các nhóm chức đặc trưng của alginate. Kết quả phân tích nhiệt trọng lượng ghi nhận quá trình mất nước tại 173,8 °C, tổng khối lượng mất đi trong quá trình nhiệt phân alginate đạt 49,65% đến 700 °C, và phần khối lượng còn lại chiếm khoảng 50%. Khả năng hấp phụ hơi nước, cho dung lượng hấp phụ cân bằng động đạt 4,22 g/g ở độ ẩm tương đối 90% và 3,84 g/g ở 70% độ ẩm, trong đó hơn 80% lượng hấp phụ được tích lũy trong vòng 15 - 20 giờ. Quá trình tái sinh nhiệt duy trì 92 - 97% dung lượng hấp phụ sau ba chu kỳ, có thể khẳng định triển vọng của vật liệu hydrogel Alg/CaAl như một loại vật liệu hấp phụ chi phí thấp cho ứng dụng thu hoạch nước từ khí quyển.

Từ khoá: Alginate; Liêt kết chéo đa hoá trị; Hydrogel; Thu hồi nước.